

https://doi.org/10.1070/QEL17640

Optical absorption in a waveguide based on an n-type AlGaAs heterostructure

Yu.K. Bobretsova, D.A. Veselov, A.A. Klimov, K.V. Bakhvalov, V.V. Shamakhov, S.O. Slipchenko, V.V. Andryushkin, N.A. Pikhtin

Abstract. **Free carrier absorption of optical radiation in layers of an AlGaAs/GaAs heterostructure is studied by the method of probe radiation coupling in order to determine the absorption cross section parameter in the AlGaAs material with a high (22%) aluminium concentration. For this purpose, we have fabricated special samples based on AlGaAs/GaAs heterostructures simulating an n-type-doped laser waveguide with carrier concentrations in the range $5\times10^{16}-3\times10^{17}$ cm^{-3}. The doping profile and the composition and thickness of layers are measured and the temperature and spectral dependences of the absorption coefficient are studied. It is shown that an increase in temperature and in the probe wavelength leads to an increase in the absorption in the heterostructure layers.**

Keywords: *semiconductor laser, semiconductor heterostructure, optical absorption by free carriers, absorption cross section.*

1. Introduction

Significant progress in the field of high-power semiconductor lasers achieved for the last decade is remarkable by record-high optical powers at high pump currents and temperatures [1]. Nevertheless, the problem of light–current curve saturation of lasers still remains topical. The main contribution to a decrease in the power and slope efficiency is mainly related to an increase in the carrier concentration and to the absorption of radiation by free carriers [2, 3]. Numerical simulation makes it possible to analyse operation of high-power semiconductor lasers with allowance for many internal processes, including free carrier absorption [4]. This requires exact knowledge of many material parameters and temperature, spectral, and other dependences. Free carrier absorption is described by cross section parameter σ. In calculations of the characteristics of InGaAs/AlGaAs/GaAs semiconductor lasers, the absorption cross sections for electrons (σ_e) and holes (σ_h) are usually taken to be (3 or 4)$\times10^{-18}$ and (10 or 12)$\times10^{-18}$ cm^2, respectively [2, 5]. These values were obtained for the GaAs material in the early days of semiconductor engineering [6, 7]. At present, most high-power lasers emitting at 900–1100 nm include AlGaAs waveguides, often with a high aluminium concentration [8–9]. The available data on free carrier absorption cross sections and their dependences on temperature, wavelength, and alloy composition for AlGaAs are not sufficiently accurate.

In our previous work [10], we proposed an original method of investigation of light absorption in heterostructure waveguides. We experimentally studied the polarisation and temperature dependences of free carrier absorption in an n-type $Al_{0.1}Ga_{0.9}As$ waveguide. The achieved accuracy of measurement of the absorption coefficient was about 0.1 cm^{-1}. This method allows one to study the absorption in various materials under different conditions (radiation wavelength and polarisation, temperature, and doping concentration). To determine the absorption cross section from experimental data, it is necessary to know the absorption coefficient, the concentration and optical field distributions in the waveguide. Therefore, to find the absorption cross section, one needs a complex approach with the use of different methods of investigation of semiconductor heterostructures.

In the present work, we continue to study the absorption coefficients in the AlGaAs/GaAs material system with n-type doping. The aim of this work is to determine the temperature and spectral characteristics of the absorption coefficient and find the absorption cross section by electrons in this material. For this purpose, we studied a series of heterostructures with different doping concentrations within the range $5\times10^{16}-3\times10^{17}$ cm^{-3}. The parameters of experimental heterostructures were extensively studied, namely, we measured the exact thicknesses and compositions of heterostructure layers, determined doping concentrations and distributions, and studied the optical absorption under different conditions.

2. Experimental samples

To perform experiments, it was necessary, similar to work [10], to fabricate special samples based on AlGaAs/GaAs heterostructures, which simulated laser waveguides. In contrast to conventional semiconductor lasers, the experimental structures have no p–n junction and active region. An $Al_{0.25}Ga_{0.75}As$ alloy was chosen as a waveguide layer. This composition is applicable for waveguides of near-IR (800–980 nm) lasers [10, 11] and lasers–thyristors [12]. In addition, we expected that the higher (than in [10]) concentration of aluminium in the waveguide layer will probably allow us to observe a stronger effect of absorption at a higher absorption cross section. The $Al_{0.25}Ga_{0.75}As$ waveguide thickness was chosen to be 3 μm both for the best wave localisation

Yu.K. Bobretsova, D.A. Veselov, A.A. Klimov, K.V. Bakhvalov, V.V. Shamakhov, S.O. Slipchenko, N.A. Pikhtin Ioffe Institute, Russian Academy of Sciences, Politekhnicheskaya ul. 26, 194021 St. Petersburg, Russia;
e-mail: nike@hpld.ioffe.ru; bobre-yulya@yandex.ru
V.V. Andryushkin ITMO University, Kronverkskii prosp. 49 A, 197101 St. Petersburg, Russia

Received 31 August 2021; revision received 7 October 2021
Kvantovaya Elektronika **51** (11) 987–991 (2021)
Translated by M.N. Basieva

in the layer of the studied material and for simpler coupling of probe radiation. To ensure optical confinement and eliminate propagation of the coupled radiation outside the waveguide, we used $Al_{0.35}Ga_{0.65}As$ cladding layers 2 μm thick each. According to the calculated mode distribution of the electromagnetic field in the heterostructure, the fraction of radiation propagating in the waveguide layer should be no less than 99%. To study the free carrier absorption due to electrons, all structures were isotypically doped with silicon. Doping concentrations for heterostructures 1–3 (HS's 1–3) (see Table 1) were $N = 5 \times 10^{16}$, 1×10^{17}, and 3×10^{17} cm^{-3}, respectively. A GaAs contact layer provided a thermal contact and the ability of soldering the samples on a carrier by a standard technique. The thickness (10 nm) and doping level (1×10^{18} cm^{-3}) of the contact layer were chosen based on the technological features of further investigation methods. The parameters for the epitaxial growth of heterostructures 1–3 are given in Table 1.

Table 1. Parameters of heterostructures (HSs) 1–3 for epitaxial growth.

Layer	Thickness	Composition	Doping
Substrate	350 μm	GaAs	N = 3 E18
Buffer layer	50 nm	GaAs	
n-cladding	2 μm	35% AlGaAs	HS 1 – N = 5 E16
Waveguide	3 μm	25% AlGaAs	HS 2 – N = 1 E17 HS 3 – N = 3 E17
p-cladding	2 μm	35% AlGaAs	
Contact layer	10 nm	35% AlGaAs	N = 1 E18

All three experimental heterostructures were grown by MOCVD (similar to the cycle for laser heterostructures) on GaAs substrates and included an $Al_{0.22}Ga_{0.78}As$ waveguide and $Al_{0.34}Ga_{0.66}As$ claddings, as well as buffer and contact GaAs layers. To verify the composition of the grown layers, the heterostructures were studied by photoluminescence (PL) spectroscopy. The PL spectra were measured at room temperature under excitation by a cw laser with a wavelength of 532 nm. The spectra were recorded using an MDR-23 monochromator and a FEU-62 photomultiplier.

Figure 1 shows the PL spectra for three heterostructures with different doping levels normalised to the PL intensity of the waveguide. The PL spectra of all three heterostructures contain two peaks at wavelength near 670 and 730 nm, which correspond to the luminescence of the $Al_xGa_{1-x}As$ material with aluminium concentrations x = 0.34 and 0.22, i.e., to the luminescence of the cladding and waveguide materials. With increasing waveguide doping level, the corresponding peak slightly shifts to longer wavelengths. Different intensity ratios of the waveguide and cladding lines are also caused by different doping concentrations. The PL signal of the waveguide in the weakly doped samples is considerably stronger than the PL signal of claddings.

The thickness of layers was verified using a Camscan 4-88-DV-100 scanning electron microscope (SEM). The real thicknesses were measured for all heterostructures. For example, Fig. 2 shows the SEM image of the end facet of heterostructure 1, which exhibits heterostructure layers with distinguishable waveguide–cladding interfaces and makes it possible to measure the layer thicknesses. The measurements show that the thicknesses of the grown layers for all heterostructures deviate from the prescribed values by no more than 10%.

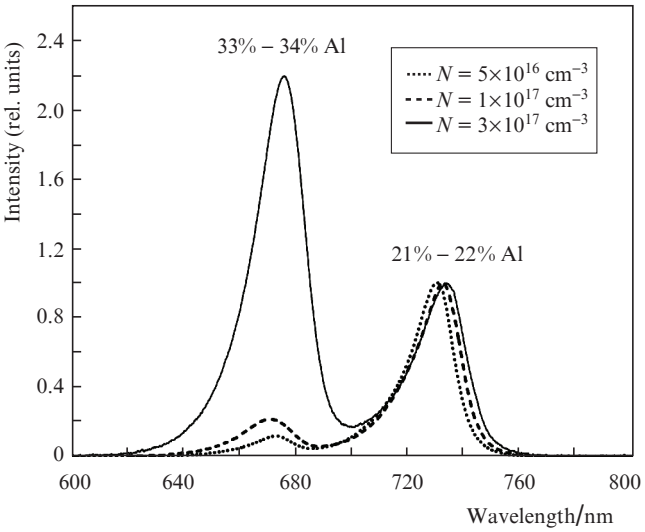

Figure 1. PL spectra of heterostructures 1–3 with different doping levels N normaliwed to the waveguide PL intensity.

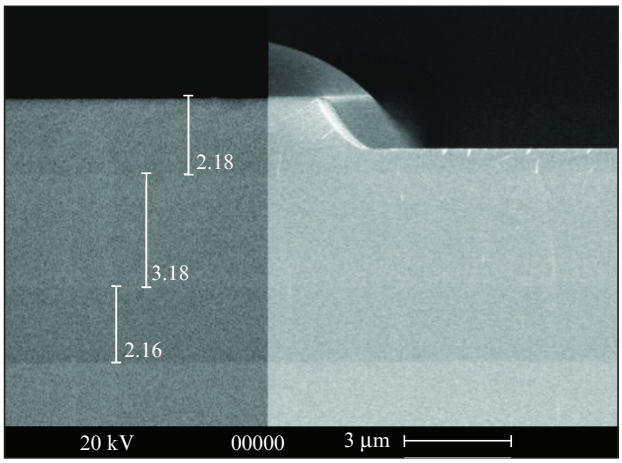

Figure 2. SEM image of the facet of heterostructure 1 (dimensions are given in micrometres).

Thus, we obtained exact parameters of heterostructures (i.e., the compositions and thicknesses of layers), which allow us to perform a comparative analysis of investigation results. For subsequent measurements of the absorption and doping concentration, we fabricated samples of different types.

The doping concentration in waveguides was measured by electrochemical capacitance–voltage (ECV) profiling. ECV profiling is based on cyclic alternation of the processes of chemical etching of the heterostructure surface and measuring of the dependence of the electrical capacitance of the barrier formed at the electrolyte–semiconductor contact on the applied bias voltage [capacitance–voltage characteristics $C(V)$]. Based on these $C(V)$ characteristics, it is possible in the depletion layer approximation to determine the free carrier concentration distribution over the thickness $N_{CV}(w)$, which coincides with the distribution of the doping concentration N [13]. Since etching of thick layers may cause inhomogeneity, the spatial resolution of the method decreases at large depths. However, this does not hinder determination of concentration in the case of uniform doping, i.e., in our

case of uniformly doped thick waveguide layers. To reduce the influence of this effect, in this work we preliminarily prepared special samples for ECV measurements. A quarter of each heterostructure wafer was stepwise etched by photolithography. Half of this quarter was covered with photoresist, and the other half was etched to a depth of about 2–2.3 μm (nearly to the waveguide). The unetched region provided an ohmic contact, while the etched region provided an electrolyte–structure contact and was used for measurements. Therefore, the concentration was controlled directly in the waveguide.

Special samples were also fabricated for investigation of absorption. In this case, heterostructures were processed via a simplified postgrowth cycle, which included only the formation of a contact from the side of layers for soldering on heat sinks and the thinning of the plate to 150 μm for convenience of its cleaving. By cleaving the plates, we obtained sets of samples with lengths of 5100, 2200, and 1500 μm. To eliminate rereflections of the probe radiation inside the crystal from the side walls, we calculated the minimum acceptable width for each length of samples [10]. As a result, we obtained sets of crystals with given lengths (5100, 2200, and 1500 μm) and corresponding widths (1500, 1000, and 500 μm). The mirrors of all samples were formed by natural cleavages without antireflective or reflective coatings. Each chip was mounted (layers down) on a carrier.

3. Investigation results

To precisely determine the doping concentration in the waveguide layer, we performed ECV profiling for each heterostructure. The concentration profiles were measured on an ECVPro profiler (Nanometrics) with the use of an electrolyte based on 10% volume fractions of ethylenediamine ($H_2NCH_2CH_2NH_2$) and Trilon-B ($C_{10}H_{14}N_2Na_2O_8$) in a concentration of 74.5 g L^{-1}. To ensure uniform etching of heterostructure surfaces, we chose an etching step of about 5 nm. Figure 3 presents the measured doping concentrations for all heterostructures. The doping concentrations in waveguides measured using ECV profiling were 5×10^{16}, 1×10^{17}, and 3×10^{17} cm^{-3} for heterostructures 1, 2, and 3, respectively. One can see that the doping distribution in the waveguide layer is uniform. In all heterostructures, the doping concentration in the claddings is higher than in the waveguide by approximately 20%. At the waveguide–cladding and cladding–substrate heterojunctions, the concentration exhibits a smooth growth with a slight slope instead of a comparatively sharp boundary expected based on the technological growth parameters, which is caused by inhomogeneous etching of heterostructure layers in the ECV method. The real concentration profile is sharper. Thus, we can conclude that the doping profile for all heterostructures turned out to be close to the desired one and rather uniform.

To study free carrier absorption, probe radiation with an exact power level polarised in the plane of the heterostructure layers was coupled through front facets into the experimental samples with different cavity lengths using an optical system. The optical power of the probe radiation passed through the sample and partially absorbed by free charge carriers inside the waveguide was measured at the output of the sample [10]. Having known a set of output powers for samples of different lengths, we can calculate the absorption inside the waveguides using the system of equations

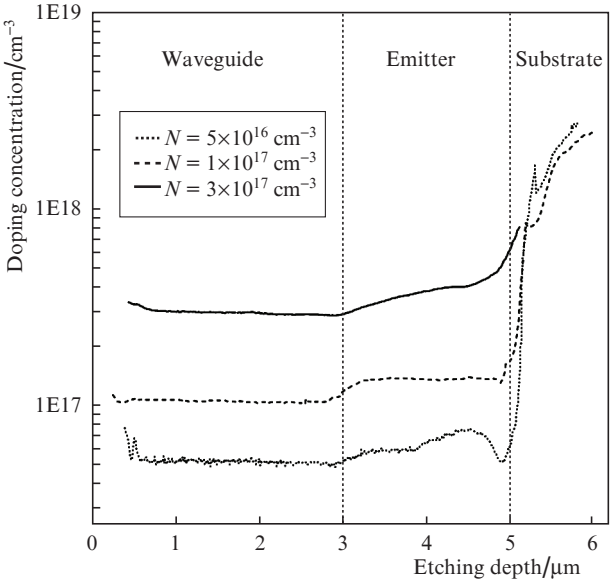

Figure 3. Doping profiles of heterostructures 1–3 measured by the ECV method.

$$\begin{cases} I_1 = \dfrac{I_0(1-R)^2\exp(\alpha L_1)}{1-R^2\exp(2\alpha L_1)}, \\ I_2 = \dfrac{I_0(1-R)^2\exp(\alpha L_2)}{1-R^2\exp(2\alpha L_2)}, \end{cases} \tag{1}$$

where I_1 and I_2 are the probe radiation powers at the output of samples with lengths L_1 and L_2, respectively; I_0 is the probe radiation power at the input to the sample; α is the absorption coefficient; and R is the reflection coefficient of mirrors. Each of the equations of the system is a sum of an infinite series {see Eqn (4) in [10]}. Thus, while in work [10] we took into account only the first five passageways of radiation through the sample, in the present work we take into account all passages. This circumstance may be important for weakly doped samples with weak absorption. Solving this system of equations, it is possible to reconstruct unknowns α and I_0. Using the calculated I_0, one can estimate the probe radiation coupling coefficient into the laser waveguide, which is important for the accuracy and reliability of the measured absorption coefficient α.

The main aim of the present work was to determine the absorption coefficient in an $Al_{0.22}Ga_{0.78}As$ waveguide as a function of the doping concentration. It was shown in [10] that absorption very slightly depends on the probe radiation polarisation, and so which all measurements were performed only for the linear radiation polarisation parallel to the plane of the heterostructure layers. The radiation power at the output of the samples was measured at temperatures in the range 25–80 °C, while the probe laser temperature was kept constant at 25 °C with an accuracy of 0.05 °C. The spectral dependence of the absorption coefficient was studied using single-mode lasers with wavelengths of 977, 1061, and 1171 nm, whose spectra are given in Fig. 4. The spectral width at half maximum for all probe lasers was about 1–2 nm. Thus, for each heterostructure, we obtained a set of powers for samples of different lengths under different conditions (temperature and probe radiation wavelength).

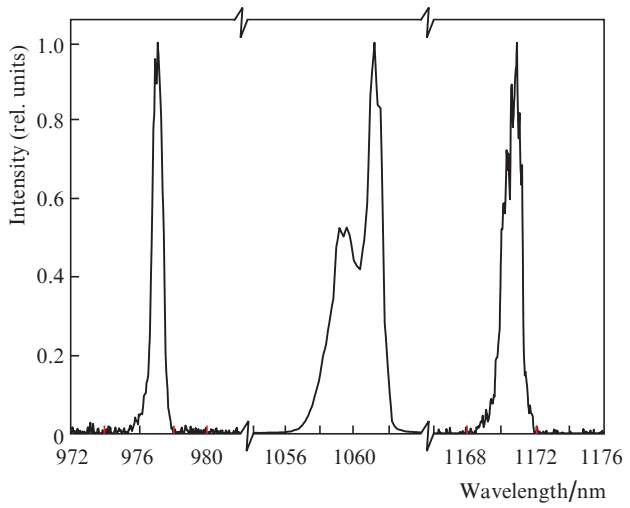

Figure 4. Emission spectra of three lasers used as sources of the probe signal.

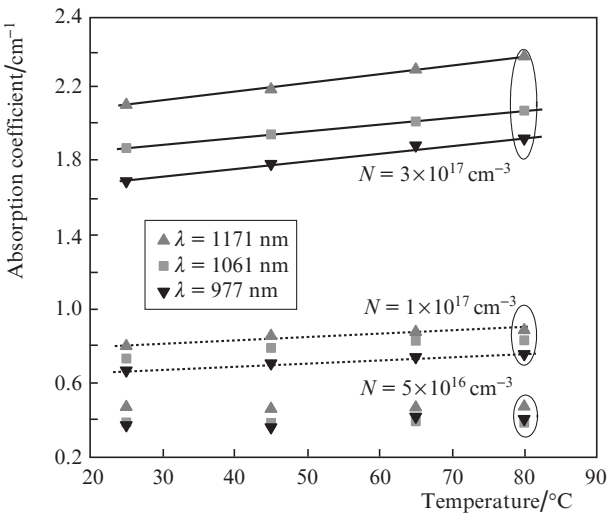

Figure 5. Temperature dependences of the absorption coefficient at wavelengths of 977, 1061, and 1171 nm for heterostructures 1–3.

Calculations by expression (1) were carried out for all pairs of samples from one heterostructure differing in lengths. The measurements were performed under identical conditions. In calculations, we used average values of powers for several samples of identical lengths under identical temperatures and wavelengths. The reflection coefficients of mirrors were calculated for each probe wavelength (977, 1061, and 1171 nm) to be 29.7%, 29.4%, and 29.2%, respectively. Similar to [10], the most accurate values of reflection coefficients were obtained for the pair of samples with the maximum difference between their lengths. For all cases, the calculated coupling coefficient was 90%–95% and almost independent of temperature and wavelength.

Figure 5 presents the temperature dependences of absorption coefficients of heterostructures 1–3 calculated for pairs of samples with lengths of 1500 and 5100 μm for all probe wavelengths. The dependences for other pairs of samples had a similar character and are not given in Fig. 5. It should be noted that the accuracy of determining absorption coefficients by this method is estimated to be about 0.1 cm^{-1}. The absorption in the waveguides with higher doping levels is proportionally higher; this allows us to suggest that the absorption is mainly caused by free carriers. Figure 5 demonstrates the existence of the temperature and spectral dependences of the absorption coefficient. The absorption for heterostructure 1, which has the lowest doping concentration, weakly depends on temperature. This may be caused, first, by the low absorption coefficient resulted in a higher relative measurement error and, second, by the fact that the contribution of the absorption by free carriers to the total optical absorption in the case of a low doping concentration can be insignificant in comparison with the contribution from other processes, for example, from scattering by heterostructure inhomogeneities. Heterostructures 2 and 3 (concentrations 1×10^{17} and 3×10^{17} cm^{-3}, respectively) exhibit noticeable temperature dependences correlating with the data obtained in [10]. Absorption in these heterostructures increases with temperature approximately linearly by 10%–15% for all probe wavelengths. Thus, at high concentrations, the contribution from the absorption by free carriers begins to dominate, and one can see a clear temperature dependence typical for this physical mechanism [14].

A noticeable increase in absorption with increasing wavelength is observed for all three heterostructures. As the wavelength increases from 977 to 1171 nm, the absorption increases by 20%–25%. In general, this temperature dependence of the absorption coefficient correlates with the data of [15]. However, due to an insufficient number of probe wavelengths and, correspondingly, experimental points, it is impossible to make a reliable conclusion about the linear of nonlinear character of this dependence.

Based on the obtained data, we can estimate the absorption cross section for each probe wavelength. It should be noted that the approach to the determination of the absorption cross section described below is applicable only for relatively weakly doped semiconductors because high concentrations of doping may lead to a deviation from the linear dependence [16].

The absorption in a waveguide is determined by the distributions of the carrier concentration and the optical field in the waveguide. In waveguide structures, the distribution of electromagnetic radiation, which sustains optical losses, is determined by the mode structure. In the general case, the absorption by electrons is described by the expression

$$\alpha = \sigma_{\mathrm{n}} \int n(x)\psi^2(x)\,\mathrm{d}x, \tag{2}$$

where $\psi^2(x)$ is the distribution of the fundamental waveguide mode intensity, $n(x)$ is the electron concentration distribution along the x axis, σ_{n} is the electron absorption cross section, and the x axis is perpendicular to the heterostructure layers [17]. Since our experiments show that the doping concentration distribution along the x axis is uniform (see Fig. 3), we can consider the dependence of free carrier absorption on the carrier concentration as

$$\alpha = \sigma_{\mathrm{n}} n. \tag{3}$$

In this case, the slope of the concentration dependence of the absorption coefficient will determine the absorption cross section. Figure 6 shows the dependences of the absorption coefficient on the doping concentration for three wavelengths of

the probe radiation measured at a temperature of 25°C. All three dependences were linearly approximated. One can see that the linear extrapolation of the obtained curves to the ordinate axis yields nonzero absorption $\alpha = 0.12$ cm^{-1}, which is independent of the doping concentration and the wavelength. We can suppose that this value corresponds to a certain constant integrated absorption, which includes effects related to structural imperfections. Thus, the absorption cross sections for the $Al_{0.22}Ga_{0.78}As$ waveguide were found to be 5.2×10^{-18}, 5.8×10^{-18}, and 6.6×10^{-18} cm^2 for radiation with wavelengths of 977, 1061, and 1171 nm, respectively. Note that the absorption coefficients of GaAs usually used in semiconductor laser physics are $(3-4) \times 10^{-18}$ cm^2 [1, 4]. In our case, the absorption coefficients are noticeably higher, which is most probably caused by high concentrations of aluminium in the waveguide composition.

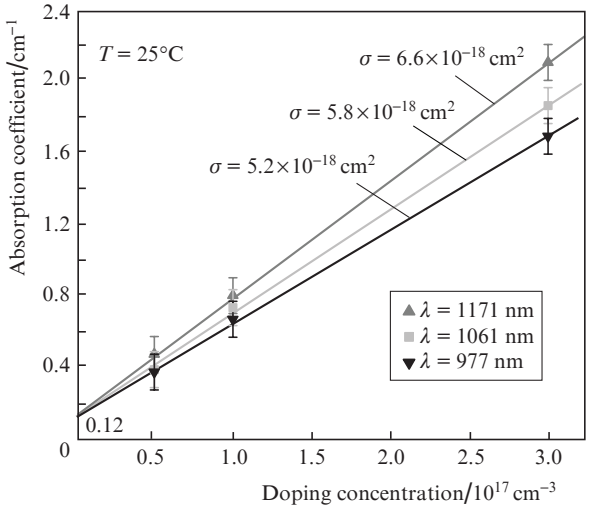

Figure 6. Dependences of the absorption coefficient on the doping concentration for three probe wavelengths at a temperature of 25 °C.

4. Conclusions

We fabricated a series of AlGaAs/GaAs heterostructures with $Al_{0.22}Ga_{0.78}As$ waveguides and different doping concentrations within the range $5 \times 10^{16} - 3 \times 10^{17}$ cm^{-3}. The technological parameters of heterostructure layers (thicknesses, compositions, and doping profiles) are confirmed experimentally. The dependences of the absorption coefficient on temperature and radiation wavelength are studied by the method developed in [10]. The optical absorption in the waveguide increases by 10%–15% with an increase in temperature from 25 to 80 °C and by 20%–25% with an increase in the probe wavelength by almost 200 nm. The absorption cross sections in the $Al_{0.22}Ga_{0.78}As$ material are determined for several wavelengths of the probe radiation. In particular, the absorption cross section for a wavelength of 977 nm was found to be 5.2×10^{-18} cm^2.

We plan to continue investigations of light absorption in semiconductor materials and to study heterostructures with different compositions of the waveguide material, as well as with different concentrations and types of dopants.

Acknowledgements. The study of the epitaxial growth of heterostructures was supported by the Russian Science Foundation (Grant No. 19-79-30072), and the experimental study was supported by the Russian Foundation for Basic Research (Grant No. 19-32-90070).

References

1. Gapontsev V., Moshegov N., Berezin I., Komissarov A., Trubenko P., Miftakhutdinov D., Berishev I., Chuyanov V., Raisky O., Ovtchinnikov A. *Proc. of SPIE*, **10086**, 1008604 (2017).
2. Piprek J. *Opt. Quantum Electron.*, **51** (60) (2019). DOI: 10.1007/s11082-019-1776-1.
3. Veselov D.A., Bobretsova Yu.K., Leshko A.Y., Shamakhov V.V., Slipchenko S.O., Pikhtin N.A. *J. Appl. Phys.*, **126**, 213107 (2019).
4. Soboleva O.S., Zolotarev V.V., Golovin V.S., Slipchenko S.O., Pikhtin N.A. *IEEE Trans. Electron Devices*, **67** (11), 4977 (2020).
5. Ryvkin B., Avrutin E. *Semicond. Sci. Technol.*, **32** (1), 015004 (2017).
6. Spitzer W.G., Whelan J.M. *Phys. Rev.*, **114** (1), 59 (1959).
7. Casey H., Panish M.B. *Heterostructure Lasers* (New York: Academic Press, 1978; Moscow: Mir, 1981).
8. Shashkin I.S., Leshko A.Yu., Shamakhov V.V., Voronkova N.V., Kapitonov V.A., Bakhvalov K.V., Slipchenko S.O., Pikhtin N.A., Kop'ev P.S. *Semiconductors*, **55** (4), 448 (2021) [*Fiz. Tekh. Poluprovodn.*, **55** (4), 344 (2021)].
9. Zhao S., Qi A., Wang M., Qu H., Lin Y., Dong F., Zheng W. *Opt. Express*, **26** (3), 3518 (2018).
10. Bobretsova Yu.K., Veselov D.A., Podoskin A.A., Voronkova N.V., Slipchenko S.O., Ladugin M.A., Bagaev T.A., Marmalyuk A.A., Pikhtin N.A. *Quantum Electron.*, **51** (2), 124 (2021) [*Kvantovaya Elektron.*, **51** (2), 124 (2021)].
11. Crump P., Wenzel H., Erbert G., Ressel P., Zorn M., Bugge F., Einfeldt S., Staske R., Zeimer U., Pietrzak A., Trankle G. *IEEE Photonics Technol. Lett.*, **20** (16), 1378 (2008).
12. Slipchenko S.O., Podoskin A.A., Rozhkov A.V., Pikhtin N.A., Tarasov I.S., Bagaev T.A., Simakov V.A. *J. Appl. Phys.*, **116** (8), 084503 (2014).
13. Ambridge T., Faktor M.M. *Electron. Lett.*, **10** (10), 204 (1974).
14. Krishnamurthy S., Yu Z.G., Gonzalez L.P., Guha Sh. *J. Appl. Phys.*, **109** (3), 033102 (2011).
15. Ryvkin B., Georgievsky A. *Semiconductors*, **33** (7), 813 (1999) [*Fiz. Tekh. Poluprovodn.*, **33** (7), 887 (1999)].
16. Pikhtin N.A., Slipchenko S.O., Sokolova Z.N., Tarasov I.S. *Semiconductors*, **38** (3), 360 (2004) [*Fiz. Tekh. Poluprovodn.*, **38** (3), 374 (2004)].
17. Ryvkin B.S., Avrutin E.A. *J. Appl. Phys.*, **97**, 123103 (2005).